



Minimum Bias Events and Missing Energy at the LHC

Dan Green

Fermilab

July, 2001

Introduction

The Large Hadron Collider (LHC) will operate at a very high luminosity. This, in turn, implies the existence of multiple minimum bias (or inclusive) inelastic non-diffractive events within the time resolution of the detectors. These “pileup” events degrade the missing transverse energy resolution with respect to that obtained for a single event. Therefore, it is important to minimize the effects of the multiple overlapping minimum bias events if that is possible.

Unfortunately, these events are dominated by strong non-perturbative interactions, which are not, in practice, calculable. Hence we must rely somewhat on the existing data from lower C.M. energy collisions. In this note a simple Monte Carlo event generator is developed which is tuned to extrapolations from the existing data.

Rapidity Distribution

Data from high energy proton- antiproton colliders has been obtained previously at several C.M. energies. The pseudorapidity distribution for produced charged particles is shown in Fig.1 [1]. Note that as the C.M. energy increases, the “width” of the “plateau” (the flat region of the distribution centered on $y = 0$) in pseudorapidity increases and the height of the plateau also increases. In the simplest models, the plateau height would be constant and the multiplicity would increase due to the lengthening of the plateau width with the logarithm of the C.M. energy.

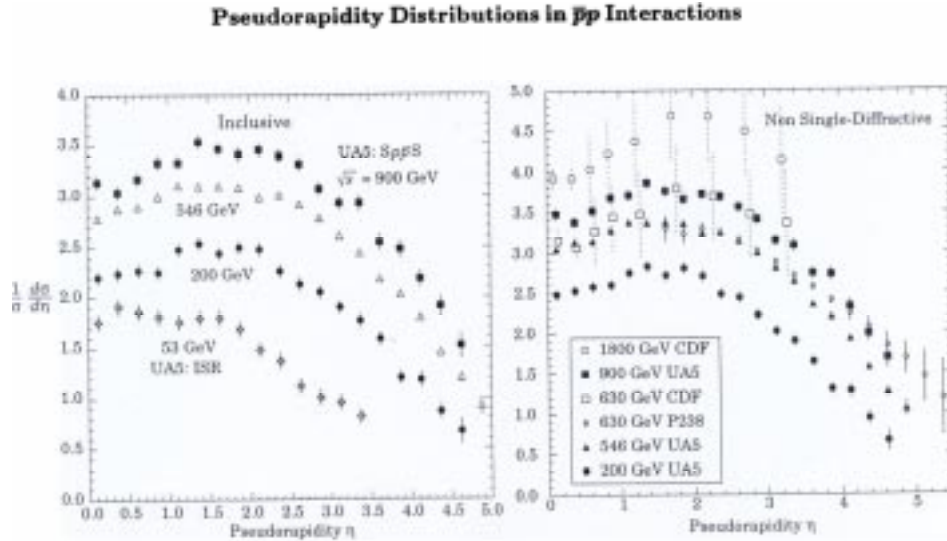


Figure 1: The distribution of the pseudorapidity of charged articles produced inclusively in inelastic proton – antiproton collisions. Also shown is the non single diffractive distribution.

Note that if the inclusive inelastic distribution were defined simply by one particle phase space, there would be a plateau which increased logarithmically with C.M. energy.

$$d^4P\delta(P^2 - M^2) = dP_t^2 dy d\phi$$

$$E = m_t \cosh(y)$$
(1)

It is clear from Eq.1 that there should be a plateau in y . Some of the data shown in Fig.1 are replotted in Fig.2 [2] where the secondary particle rapidity is referred to the beam rapidity, which is roughly the maximum rapidity an emitted secondary particle can have. A “scaling” behavior is observed. The distribution in pseudorapidity less the beam value is independent of C.M. energy for values of pseudorapidity, η , near that of the incident beam. We will assume this behavior is constructing the Monte Carlo model.

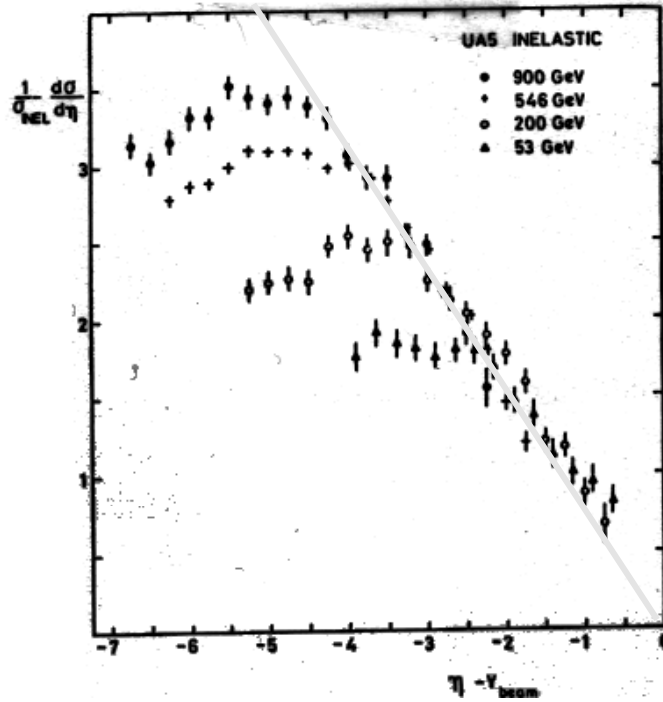


Figure 2: Distribution of charged particle pseudorapidity for different beam energies showing “scaling” of the distribution after the “plateau” has fallen off. A simple linear dependence is a decent description of the dependence of the data.

This behavior can be extrapolated to the LHC. A plot of the beam rapidity vs. the density of emitted charged particles on the plateau is shown in Fig. 3. Clearly, a plausible extrapolation to the LHC gives a range of from 5.0 to 6.0 charged particles per unit of rapidity. Assuming pion emission dominates, that means 7.5 to 9.0 pions (positive, negative and neutral) emitted per unit of rapidity on the plateau.

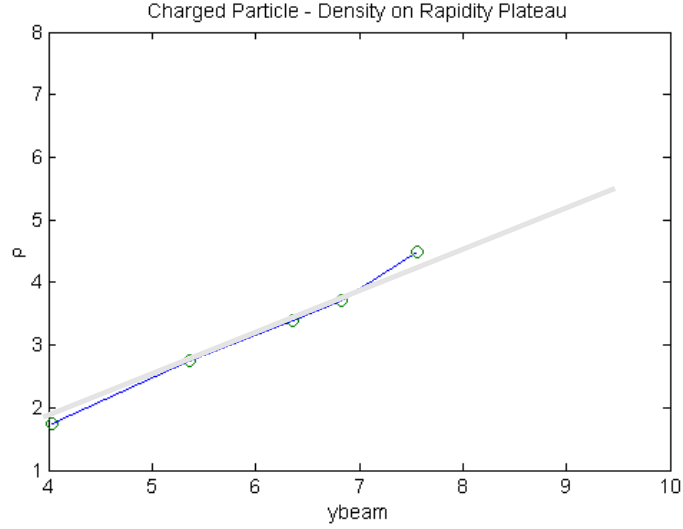


Figure 3: Extrapolation of data taken from Fig.1. The beam rapidity is plotted against the density of emitted charged particles on the plateau. The LHC beam rapidity is 9.6.

A simple Monte Carlo model was written to simulate minimum bias events. For the rapidity, particles were produced with the inclusive distribution. The distribution was taken to be defined by the shape. There was a plateau out to y_{roll} , followed by a linear (see Fig.2) falloff from the plateau to the beam rapidity. Using the data of Fig.2, a plausible extrapolation of y_{roll} to the LHC would place y_{roll} in the range from 2.7 to 1.5. The resulting Monte Carlo distribution for the pion rapidity is shown in Fig.4.

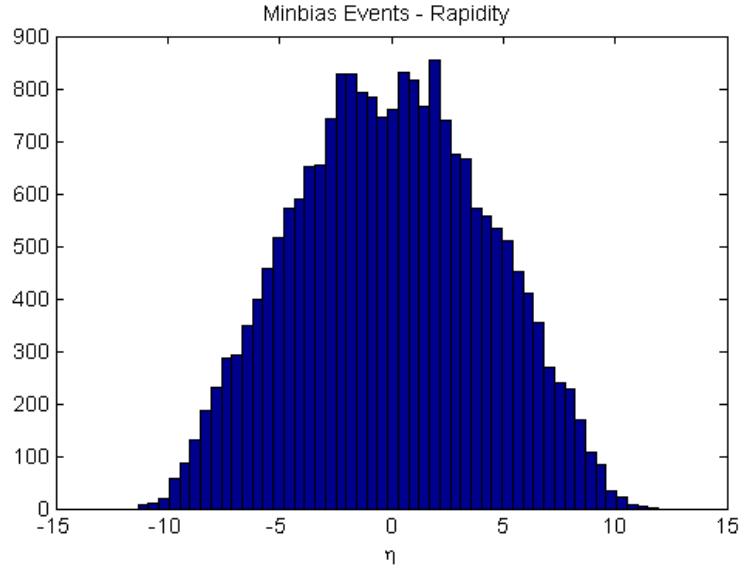


Figure 4: The Monte Carlo distribution for pions used in this work. It is characterized by a single variable, y_{roll} which is the boundary between the plateau and the linear falloff to zero at the beam rapidity. The value of y_{roll} was taken to be 2.2 for this set of events.

Transverse Momentum Distribution

For the purposes of this simple model we assume that the rapidity and the transverse momentum distributions factorize. This is known to be roughly true from examination of the lower energy data [2]. The distribution of the mean transverse momentum of the emitted charged secondary particles [2] is shown in Fig.5. Clearly, the extrapolation to the LHC is not very obvious. Average values of transverse momentum might vary from 0.5 to 0.65 GeV at the LHC.

For the Monte Carlo generation of transverse momentum (Pt) we used a simple distribution. The square of the transverse momentum was distributed as an exponential characterized by a single variable. That variable was adjusted to give the appropriate mean value of Pt. The resulting transverse momentum distribution is shown in Fig.6.

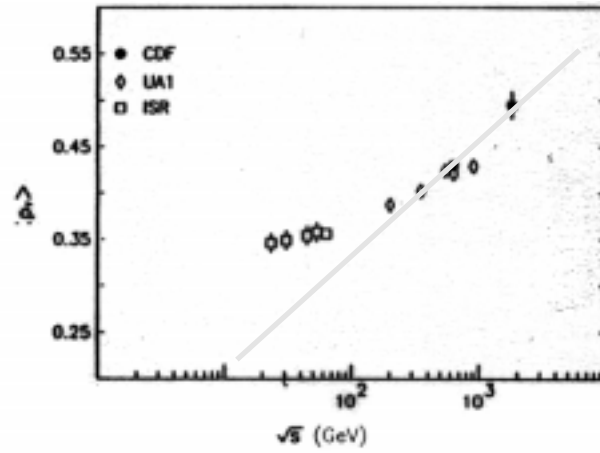


Figure 5: Data on the average transverse momentum of secondary charged particles as a function of C.M. energy from experiments at lower energy than the LHC.

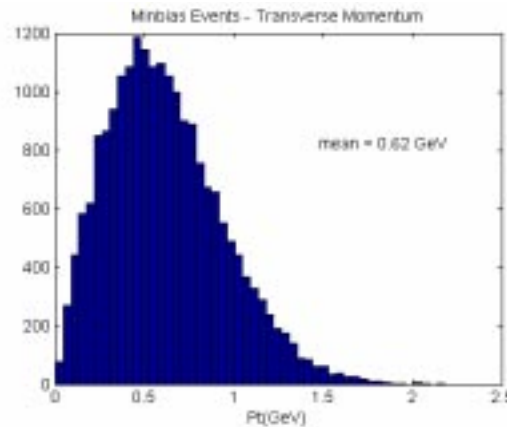


Figure 6: Distribution of transverse momentum for the produced pions in the Monte Carlo model. The single parameter defining the distribution has been adjusted so that the mean value of Pt is 0.62 GeV.

Multiplicity Distribution

Data on the multiplicity of emitted charged particles is shown in Fig. 7. Note the logarithmic rise of the mean charged multiplicity with C.M. energy. Extrapolating to the LHC, we expect a charged multiplicity in the range 45 to 65 or a total emitted pion multiplicity of 65 to 100. As was the case with Pt, the validity of a logarithmic extrapolation is not obvious.

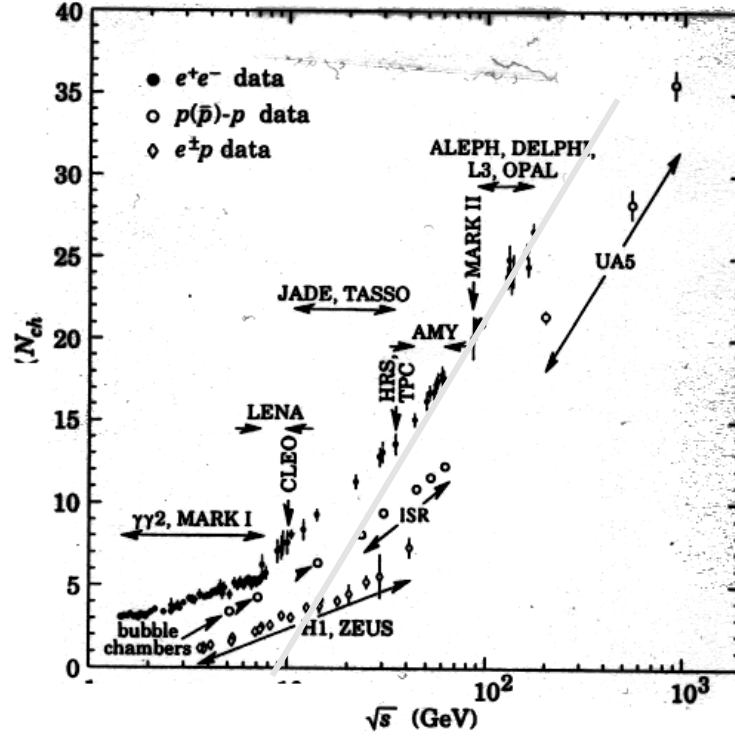


Figure 7: Data on the mean multiplicity of charged secondary particles as a function of C.M. energy.

The simple model we have constructed has only two variables. Pions are picked out of factorized rapidity and transverse momentum distributions as described above. The former is defined by a single variable, y_{roll} , which defines the extent of the rapidity plateau. The latter is defined by a single variable which defines the mean transverse momentum, $\langle Pt \rangle$. The pions are picked until the total C.M. energy is reached. Therefore, the pion multiplicity and the density of emitted pions on the plateau are not independent adjustable variables in this simple model. In fact, with a density of 7 on the plateau and a linear falloff from $|y| = 2$ to $|y| = 10$, we expect a multiplicity of ~ 84 . Note that there are no explicit correlations between secondary particles.

The value of y_{roll} was taken to be 2.2, consistent with an extrapolation of the data shown in Fig. 2. The mean transverse momentum was adjusted to be 0.62 GeV, consistent with the extrapolation of the data shown in Fig. 5. The resulting multiplicity of pions in this model is shown in Fig. 8. The mean is $\langle n \rangle = 104$, consistent with data extrapolations taken from Fig. 7.

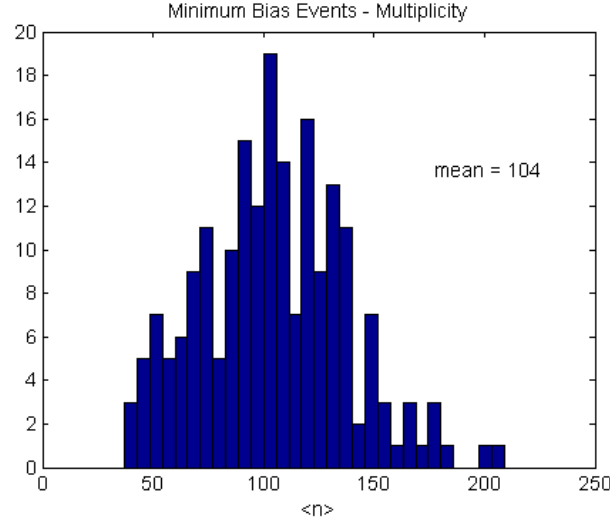


Figure 8: Monte Carlo model results for the distribution of pion multiplicity at the LHC.

The density of emitted pions can be taken from the distribution given in Fig. 4. The observed value is 7 pions emitted per unit of rapidity. This value is consistent with, but on the low end of the extrapolation of the data shown in Fig.1 and Fig.2. Higher values of the density can be obtained by reducing y_{roll} , which shortens the plateau and raises it. That, in turn, changes the multiplicity distribution. Lowering the value of $\langle Pt \rangle$ also increases the density because the number of pions is set by energy conservation. As a numerical example, taking $y_{\text{roll}} = 5$ and $\langle Pt \rangle = 0.80$ GeV we find $\langle n \rangle \sim 80$ and a plateau density ~ 5 .

The missing transverse momentum in the minimum bias events is caused by incomplete angular coverage, the sweeping effects of the magnetic field, and the energy errors inherent in the calorimetric measurement of energy. The Monte Carlo program described here creates events which explicitly conserve transverse momentum and longitudinal energy. The conservation of longitudinal momentum is imposed up to small effects of pion masses. In addition, jets can be added to the events. These jet pairs are emitted at 90 degrees in the C.M. and conserve all three components of momentum. We use these events to study the contributions to missing transverse momentum.

Effect of Angular Acceptance

The incomplete angular coverage of experiments at the LHC is an experimental necessity due to the very large radiation field at small angles and the vacuum beam pipes which limit detector coverage. A typical maximum pseudorapidity coverage is up to 5. We study each of the three effects with the others turned off. The missing transverse energy is defined using the sum of E_x and E_y over all secondary particles to be the square root of the sum of the squares.

Minimum bias events were generated and the energy was assumed to be undetected if $|y| > y_{\text{max}}$. The results are shown in Fig.9 for the missing transverse energy as a function of y_{max} . The missing energy is defined to be the total detected vector transverse energy. Clearly if $y_{\text{max}} = 0$,

that energy is zero since none is detected. If $y_{\max} \sim 9.6$, then all the energy is detected and again the missing energy is zero. In between, the value of y_{\max} from 3 to 7 is quite constant. Therefore, in the LHC experiments, the coverage was chosen to accept the desired high Pt physics signals rather than to minimize the missing transverse energy. At a maximum y of 5, the effect of limited coverage alone is to induce a missing Pt of 5.2 GeV.

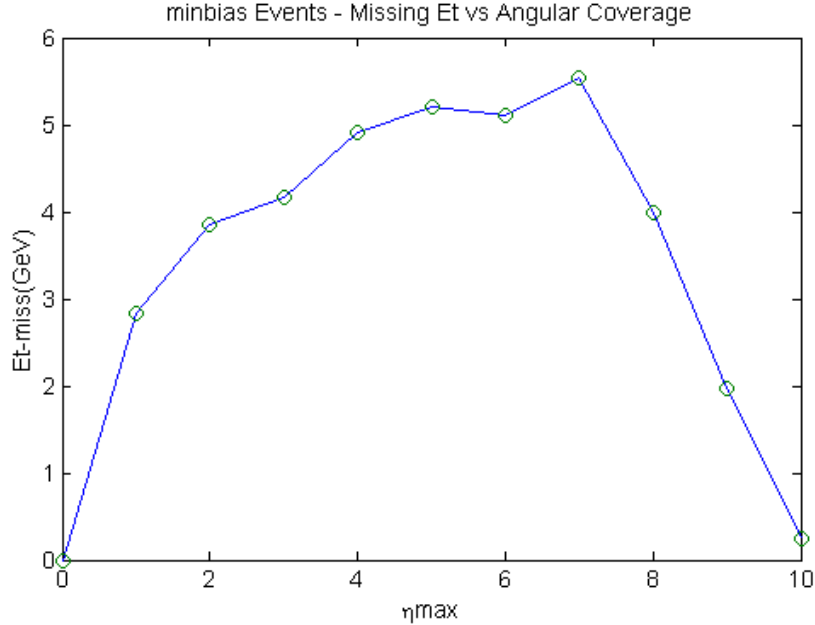


Figure 9: The missing transverse energy as a function of the rapidity of the total angular coverage of the LHC detector.

Effect of Magnetic Field

The magnetic field induces a missing transverse energy if the calorimeter is used to define energies. That is because the charged particles are rotated clockwise or anti-clockwise in azimuth in traversing the volume between the event vertex and the calorimetry. These rotations are governed by the charge of the emitted pions. Note that in an extreme case a charged pion emitted at 90 degrees may be swept from the barrel down to the endcap and misassigned in angle inducing a large error in transverse momentum. For example, in CMS any charged track emitted toward the barrel (wide angles) with a $P_t < 1.1$ GeV is swept into the endcap and assigned a small angle. As the energy remains the same the P_t assigned by the calorimetry is much underestimated.

Monte Carlo events were generated and charged particles were propagated to the exit points of a closed cylinder which was used to approximate the front faces of the CMS barrel (wide angle) and endcap (small angle) calorimeters. These impact points were used to define calorimeter derived values of rapidity, azimuthal angle and transverse momentum. The rapidity distribution derived from calorimetric measurements is shown in Fig. 10. Note the severe depopulation of the barrel region.

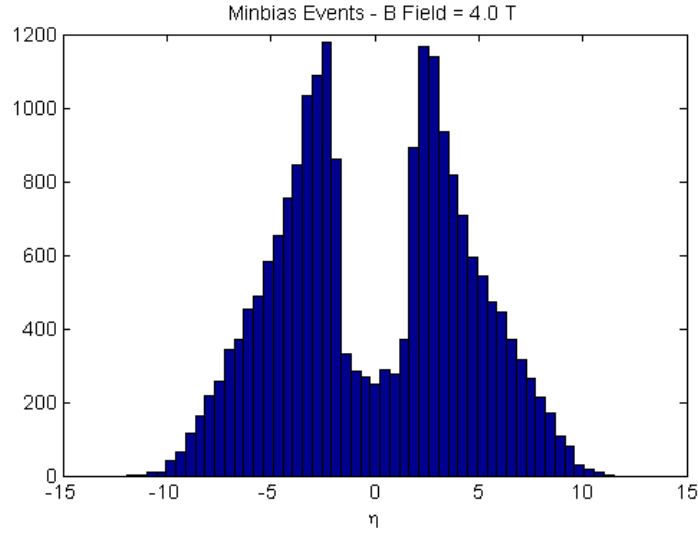


Figure 10: Rapidity distribution based on particle impact points in the CMS calorimetry.

The only remaining hits in the barrel region are due to undeflected neutral pions and high Pt charged pions. A scatter plot of the rapidity and Pt derived from the calorimeter impact point information is shown in Fig. 11. Note the strong sweeping effect where particles emitted at $y \sim 0$ are swept by the magnetic field into small angles. At wide angles there is a smattering of low Pt neutral pions. At wide angles and high Pt (> 1.1 GeV) a fairly uniformly distributed plateau is recovered. The effect of the magnetic field alone is fairly linear, inducing a missing transverse momentum of ~ 1.1 GeV/Tesla, or 3.46 GeV at design field of 4 T.

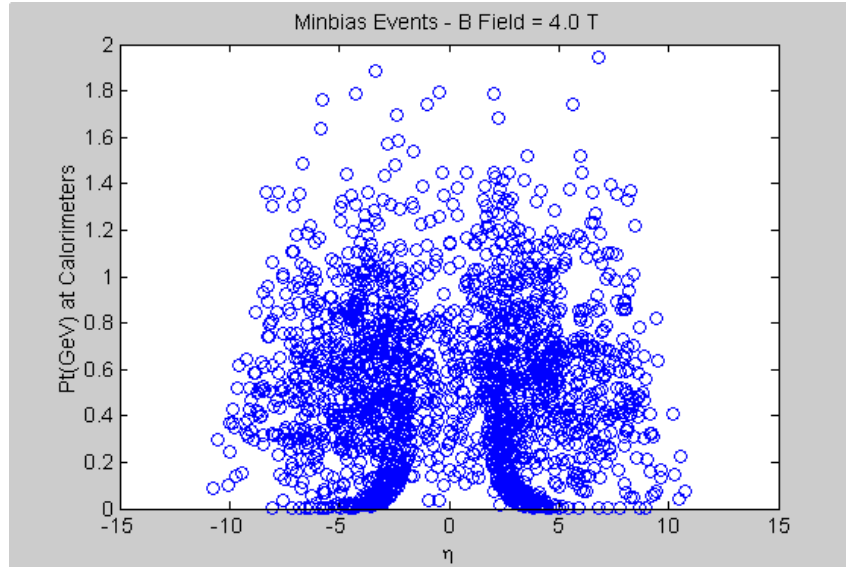


Figure 11: Scatter plot of y vs. Pt where the kinematic variables are derived from impact points and energy measured in the calorimetry. The calorimetry is approximated to exist as a cylindrical barrel closed off by circular endcaps. The barrel/endcap transition occurs at $|y| \sim 1.5$

Effect of Total Et in the Event

The final effect which was studied was the assumed calorimetric energy resolution. The fractional resolution in energy was assumed to be uniform with dE/E possessing a stochastic coefficient of 100 % and a constant term of 3%.

$$dE/E = 1.0/\sqrt{E} \oplus 0.03 \quad (2)$$

The effect of calorimeter resolution alone is shown in Fig. 12. The events used were minimum bias events with dijets of a fixed PtJ overlapped. The plot is the missing transverse momentum as a function of the total jet transverse momentum in the event. In the absence of jets, the mean missing Pt is 2.35 GeV. The mean missing Pt rises with the Pt of the overlapped jets.

$$\langle Et \rangle \sim 0.48\sqrt{\sum Et} \quad (3)$$

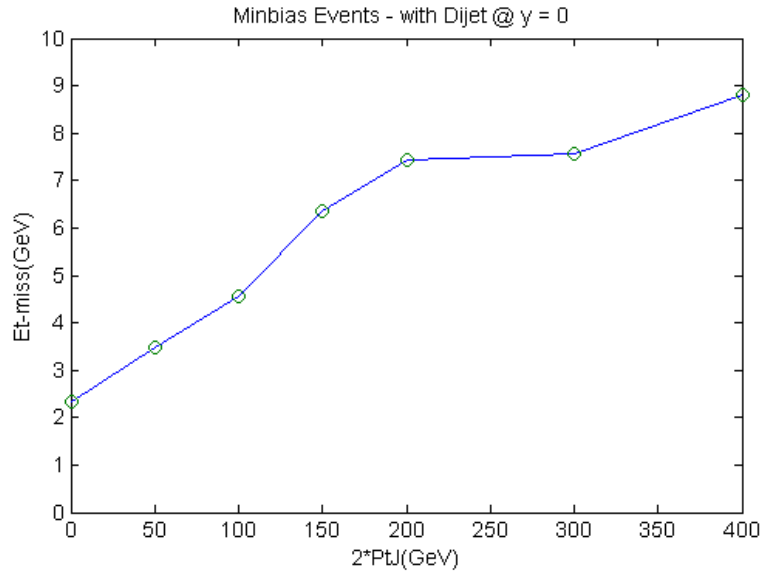


Figure 12: Missing transverse momentum in minimum bias + dijet events with only the effect of calorimetric energy resolution turned on. For high Pt dijets, the x axis is approximately the total scalar sum of the transverse energy in the event.

Summary and Conclusions

The combined effect of the incomplete angular coverage, the magnetic field, and the calorimetric energy resolution is shown in Fig. 13. The mean value of the missing transverse energy in a minimum bias event is 5.02 GeV in this simple Monte Carlo model of minimum bias events. Note that the result of folding the three effects in quadrature yields 6.7 GeV, so it appears that the effects are not completely independent.

For example, the mean scalar sum of Pt in an event is 61.6 GeV within $|y|$ of 5 if the magnetic field is off. Turning the field on sweeps secondary particles toward the endcaps, lowering the measured Pt in the calorimeters. For the full CMS field of 4 T, the mean scalar Pt is reduced to 57 GeV.

It appears that, with the chosen extrapolation of existing data defined in this paper, that the CMS calorimetry does not drive the missing energy resolution. It is, indeed, the smallest effect. The effect of magnetic field can be partially alleviated if the CMS tracker is fully efficient. In that case, the charged tracks can be assigned their vector momenta at the production vertex. If this is possible, the magnetic field effects can be reduced to a low value. In addition, using the momentum found in the tracker, the effect of calorimeter resolution can be greatly reduced for charged tracks. Recall also that the CMS electromagnetic calorimetry has a very good energy resolution. Therefore, the missing transverse momentum due to calorimeter resolution and magnetic field sweeping can, in principle, be made negligible.

This leaves the dominant effect due to incomplete angular coverage. Clearly, looking at Fig.9 the exact size of the effect depends on the shape of the falloff from the rapidity plateau. In any case, the experimental constraints due to the high radiation field at small angles probably makes it impossible to imagine a calorimeter operating at values of $|y| > 5$. For example, the $|y| \sim 5$ boundary in CMS has calorimetry which absorbs a dose of ~ 1 Grad over 10 years of LHC operation. In addition, the size of hadronic showers at small angles begins to be comparable to the size of a jet. Therefore, the ability to measure the energy flow with good resolution in y is badly compromised at large $|y|$. Moving the calorimetry away from the interaction point eases this problem. Indeed, that is why in CMS the forward calorimeter was placed twice as far downstream as the endcap. Even so, at $|y| \sim 5$ the calorimeter towers large, $dy \sim 0.5$, because the hadronic shower is of comparable size.

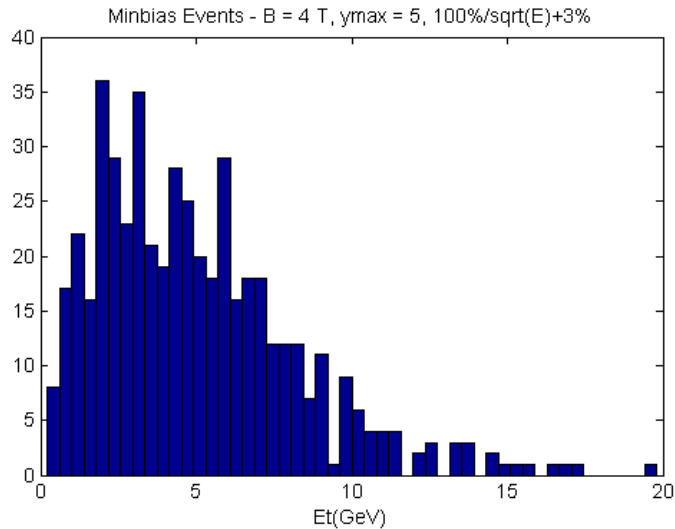


Figure 13: Missing transverse momentum induced in a single minimum bias event due to incomplete angular coverage, magnetic field sweeping, and calorimetric energy resolution.

References

1. Particle Data Group, Review of Particle Physics (2000)
2. Topical Workshop on Proton-Antiproton Collider Physics, World Scientific, 20-24 June, 1988.